Nonlocal Nonlinear Electro-Optic Phase Dynamics Demonstrating 10 Gb/s Chaos Communications

R. Lavrov, M. Jacquot, L. Larger

Nonlocal Nonlinear Electro-Optic Phase Dynamics Demonstrating 10 Gb/s Chaos Communications

Roman Lavrov, Maxime Jacquot, and Laurent Larger, *Member, IEEE*

***Abstract*—We report on successful 10 Gb/s transmission of a message hidden in a chaotic optical phase over more than 100 km of an installed fiber optic network. This represents the best performance to date for so-called optical chaos communication, a physical layer oriented optical data encryption technique. Such performances was achieved through the use of a recently developed electro-optic nonlinear delay phase dynamics, inspired from differential phase modulation techniques. The setup appears as a superior alternative to the most popular architectures, i.e., the ones involving laser rate equations subjected to delayed feedback. It is compatible with standard dispersion compensation techniques and optical amplification, as shown by two field experiments over installed fiber optic networks.**

***Index Terms*—Chaos synchronization, electro-optic (EO) feedback, nonlinear delay dynamics, optical chaos communications, optical phase modulation.**

I. Introduction

SINCE the first demonstration of chaos synchronization 20 years ago [1], chaotic dynamics in photonic systems has been intensively explored as a means of providing enhanced physical layer data protection in optical communications [2], [3]. Although many popular setups are based on the nonlinear chaotic behavior of semiconductor lasers subject to electrical or optical feedback [4]–[11], this approach is currently limited to transmission at bit rates of 2.5 Gb/s and requires additional software-level error correction to obtain link quality compatible with practical system demands [12]. On the other hand, chaos communications based on electro-optic (EO) feedback has been studied and demonstrated as an alternative approach and indeed has been successfully used in field experiments at comparable bit rates through optical intensity modulation [11]. In this article, we report on the experimental results of a new approach to optical chaos encoding and decoding, involving an original architecture performing temporally nonlocal nonlinear delayed EO phase modulation [13]. Thanks to the efficiency of the proposed approach, we could perform the first experimental demonstration of 10 Gb/s chaos communication over installed fiber optic networks. In conclusion, we anticipate that the proposed setup and its attractive and controllable dynamical features, are not limited to chaos communications, being also of interest in future real time and fast optical processing systems, such as synchronizable random number generation, or optical processing in reservoir computing.

The authors are with the Optics Department of the FEMTO-ST Institute, University of Franche-Comté, Besançon 25030, France (e-mail: r.lavrov@gmail.com; mjacquo6@univ-fcomte.fr; laurent.larger@univ-fcomte.fr).

II. EO Setup

The setup depicted in Fig. 1 shows the emitter-receiver architecture of the phase chaos communication system. It consists first of a standard communication link based on differential phase shift keying (DPSK) modulation. Note that any wavelength division multiplexing (WDM) channel can thus be selected through the use of the proper external laser source, independently of the subsequent chaos communication processing. A message phase modulator MΦM performs the binary DPSK phase modulation φ_m corresponding to the message to be transmitted. It is worth noting here that MΦM could be equivalently placed before seeding the chaotic oscillator, or inside this oscillator. The chaotic masking is indeed consisting in the superposition of the message phase modulation, and the chaotic masking phase modulation, the latter being thus partly determined also by the message phase modulation. If the message phase modulation had been performed after, and outside, the oscillation loop, the chaotic masking would be independent of the message phase modulation. The chaos encoding technique we used is thus of the same kind as other earlier published in-loop addition approaches [2], [3], [14]. The phase chaos generator (ΦCG) [13] thus performs the masking of the DPSK message. At the receiver side, phase chaos cancellation (ΦCC) is processed from the input light beam, after which a standard DPSK demodulation MΦD recovers the original binary message. Note that if ΦCG and ΦCC are deactivated, the communication link becomes a standard optical DPSK transmission (chaotic masking and unmasking can thus be switched on and off).

A brief description of the novel chaos generation process at the emitter is as follows. The dynamics belongs to the class of nonlinear delay differential equations, which were popularized in the wider scientific literature, e.g., by Mackey and Glass in the life sciences [15], and by Ikeda in optics [16]. According to the initial idea of the Ikeda dynamics, a nonlinear transformation is performed while modulating the phase condition in an interferometer. Instead of implementing

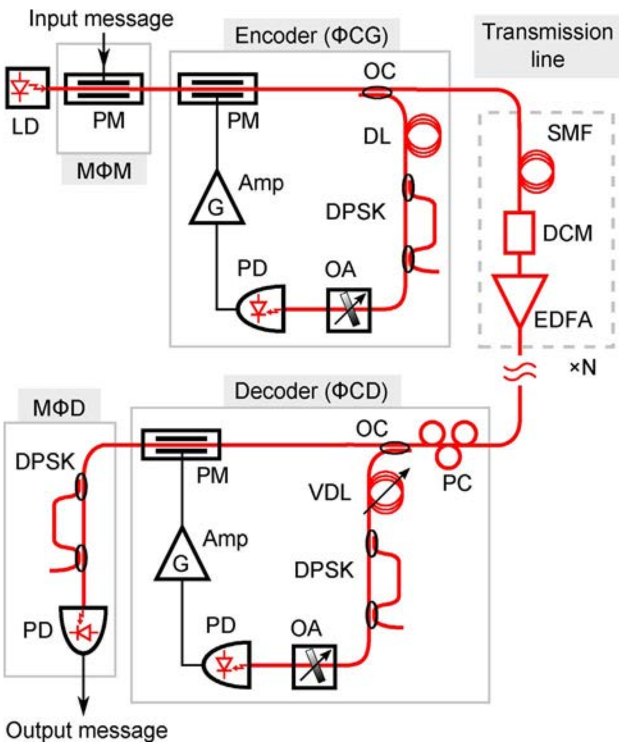

Fig. 1. Point-to-point transmission setup using EO phase chaos. Transmitter performs standard DPSK binary message modulation (MΦM) and chaotic phase masking (ΦCG). The phase modulated light beam is sent to the receiver through an installed network fiber link. The receiver performs first the chaos cancellation or demodulation (ΦCD) through phase chaos synchronization, and then standard DPSK demodulation retrieves the binary signal in the electrical domain (LD: laser diode, PM: phase modulator, DPSK: differential phase shift keying demodulator, OA: optical attenuator, PD: photodiode, Amp: telecom driver, OC: optical coupler, SMF: single mode fiber channel, EDFA: erbium doped fiber amplifier, DCM: dispersion compensation module, PC: polarization controller, VDL: variable delay line).

this interferometer with an EO Mach-Zehnder [14], [17], the interferometer function and the phase modulation operation are split (see ΦCG in Fig. 1). The actual interferometer is imbalanced with a delay δT, leading to an interference condition ruled by the phase difference between times t and $(t-\delta T)$. As soon as the EO phase modulation is performed faster (response time τ) than the time imbalancing ($\delta T \gg \tau$), a dynamic scanning of the nonlinear interference modulation transfer function is achieved. This modified Ikeda dynamics is inspired by conventional DPSK modulation and demodulation techniques. Notice however that *a priori* any multiple wave imbalanced interferometer can be used as a "hardware key" determining the chaos generation process.

A general formulation of this nonlinear function can be written as follows:

$$f_t(\varphi) = F_0 \left| 1 + \sum_k \alpha_k \, e^{i[\varphi(t)-\varphi(t-\delta T_k)]} \, e^{i\phi_k} \right|^2 \qquad (1)$$

where δT_k is a time imbalance with respect to a reference arm, α_k is its relative amplitude weighting, ϕ_k defines its static offset phase, again with respect to a reference arm, and F_0 is an arbitrary amplitude normalization factor. Equation (1) defines the temporally non local non linearity involved in the dynamics. In the phase chaos communication demonstrator described here, we practically use a commercial two wave unbalanced interferometer consisting of a fiber based 2.5 GHz Mach-Zehnder DPSK demodulator. This leads to $k = 0$ only, $\delta T = \delta T_0 \simeq 400$ ps, $\alpha_0 = 1$, and ϕ_0, and thus $f_t(\varphi) = \{1 + \cos[\varphi(t) - \varphi(t-\delta T) + \phi_0]\}$ (with $F_0 = 1/2$). The differential process ruling the chaotic dynamics is derived from the bandpass filtering performed by the optoelectronic feedback path (from the photodiode to the EO electrodes, see [14] for additional details). Such a filter can be approximated by only two low and high cut-off frequencies, corresponding to an integral response time θ (slow time scale of a few μs), and a differential response time τ (fast time scale of a few 10 ps), respectively. This leads to the following integro-differential delay equation:

$$\frac{1}{\theta}\int_{t_0}^{t} \varphi(\xi)\mathrm{d}\xi + \varphi(t) + \tau\frac{\mathrm{d}\varphi}{\mathrm{d}t} = \beta \cdot [\, f_{(t-T)}(\varphi^\star) - f(0)] \qquad (2)$$

where T stands for the total time delay involved in the feedback loop, and β is a normalized feedback gain of the delayed nonlinear feedback. The variable $\varphi^\star = \varphi + \varphi_m$ describes the impact of MΦM on the chaotic motion: it is injected into ΦCG, as an additional binary phase modulation. This message phase modulation is linearly superimposed to the chaotic masking signal through the serial configuration of the two phase modulators. The message to be hidden inside the chaotic masking signal, is thus also contributing to this chaotic signal itself (scheme sometimes referred as "chaos embedded message"). This particular mixing process between the message and the chaos has the advantage of mutual masking such that each signal hides the other: the chaotic signal is hiding the message as expected, but the message is also perturbing the original message-free deterministic dynamics. The presence of the message is blurring an eventual deterministic cryptanalysis of the chaotic motion by an eavesdropper. Cryptanalysis of time delay chaotic waveforms is commonly explored in a message-free configuration, for which the time series are purely deterministic, and thus easier to analyze [18]. The presence of a strong enough random message is here expected to prevent, or at least to complicate, the usual identification techniques for delay dynamics.

III. Chaos Communications Results

Fig. 2(a) shows the rf spectrum evolution of the differential phase dynamics without a message, as β is increased from 0, to the maximum experimentally achievable value (ca. 5). The route to chaos of delay dynamics is typically going from the stable steady states (low β), to the fully developed chaos (high β), through periodic and quasi-periodic oscillations (intermediate β). The chaotic motions are obtained already at $\beta = 2$ in a message-free operation, however revealing in its rf spectrum some characteristic frequencies related to $1/(2\delta T)$. The strongly chaotic regimes obtained for $\beta = 5$ exhibit a nearly flat and white noise-like rf spectrum, over the full bandwidth of the oscillator (ca. 30 kHz–13 GHz). In the presence of a binary message, a strong flatening of the rf spectrum is observed, already at $\beta = 2$.

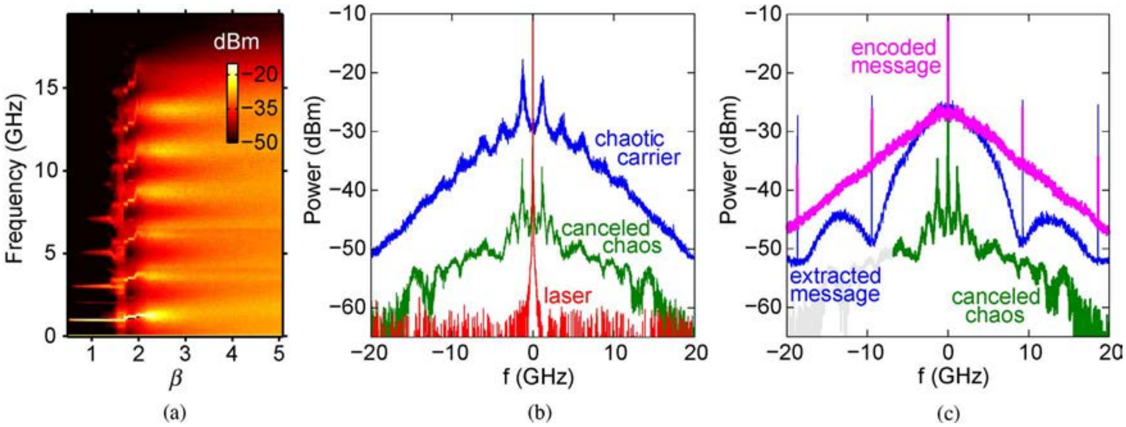

Fig. 2. Experimental spectral characteristics. (a) Spectral (electrical domain) chaotic distribution vs β. (b) Chaotic carrier and chaos cancellation spectra together with unmodulated laser. (c) Encoded and extracted message on top of the cancellation spectrum.

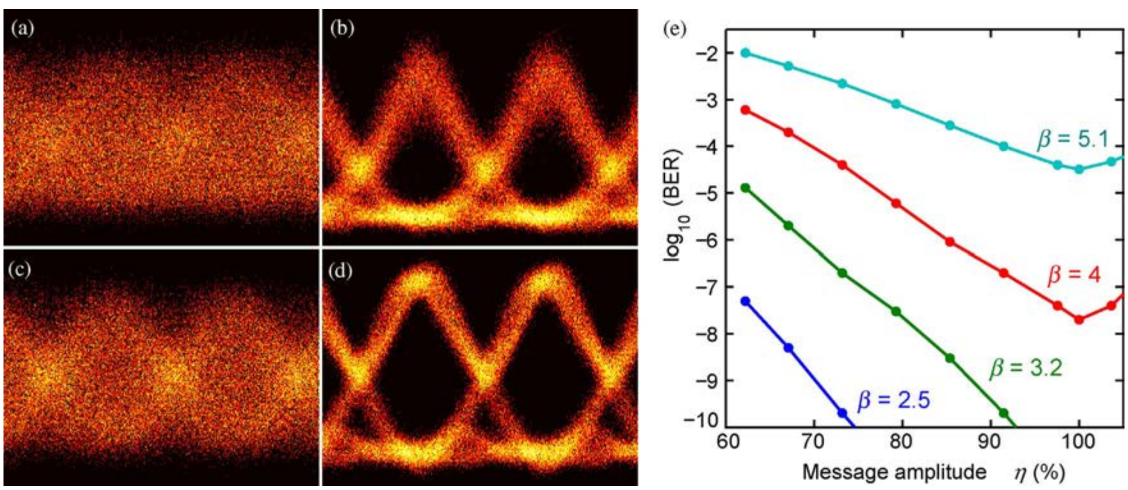

Fig. 3. 10 Gb/s back-to-back experimental results. Eye diagrams for [(a) and (c)] unauthorized (direct detection) and [(b) and (d)] authorized receiver for different message amplitudes. (a) and (b) η = 60%. (c) and (d) η = 100% at β = 4. (e) BER dependence on message amplitude for an authorized receiver for different β values.

At the receiver side, phase chaos cancellation is achieved using the so-called open loop receiver scheme: the receiver is aimed at replicating the emitter nonlinear delay processing path (with a minus sign). At the end of this path, the receiver EO phase modulation is applied onto the incoming light beam, with the aim of suppressing the chaotic masking phase modulation performed at the emitter. Due to the anti-phase replicated nonlinear delayed processing, the receiver phase modulation is ruled by a similar equation to (2)

$$\frac{1}{\theta'}\int_{t_0}^{t}\varphi'(\xi)\mathrm{d}\xi + \varphi'(t) + \tau'\frac{\mathrm{d}\varphi'}{\mathrm{d}t} = -\beta'\cdot[f'_{(t-T')}(\varphi^\star) - f'(0)] \tag{3}$$

where symbol "′" denotes the parameters or functions involved at the receiver, similar to the ones at the receiver, but slightly different due to unavoidable parameter mismatch. The drive signal $\varphi^\star$ is the same as the one at the emitter. Notice that the minus sign of β' can be obtained experimentally when exchanging the inputs of a balanced detector, or when using the complementary outputs of the DPSK demodulator, or also when adjusting the receiver phase ϕ'_0 in quadrature with respect to the emitter value ϕ_0. Chaos cancelation at the output of the receiver phase modulator, is successfully achieved as illustrated by Fig. 2(b), when all receiver parameters are matched as closely as possible with the ones set at the emitter. This chaos cancelation is obtained according to the principles of the open loop receiver already described in [14]. The stability of the synchronization manifold can be derived when adding (through serial additional phase modulation at the receiver) (3) and (2), resulting in the dynamics of the synchronization error $\varepsilon = \varphi + \varphi'$. The zero fixed point solution for this error ($\varphi' = -\varphi$) is found to be stable, resulting in a synchronized receiver, and thus in a canceled chaotic phase modulation after the EO phase modulator at the receiver.

Fig. 2(b) shows the optical spectrum of the experimental residual phase modulation, which is remaining after chaos cancellation due to residual parameter mismatch (without message) [19]. The embedding chaotic spectrum is superimposed on that figure: the gap between the two spectra (upper blue curve and middle green curve) represents the space where a message can be encoded, and decoded. The gap has approximately a 10 dB vertical optical height (20 dB electrical), at least over $\pm$10 GHz side bands, as expected when using 10 Gb/s qualified devices.

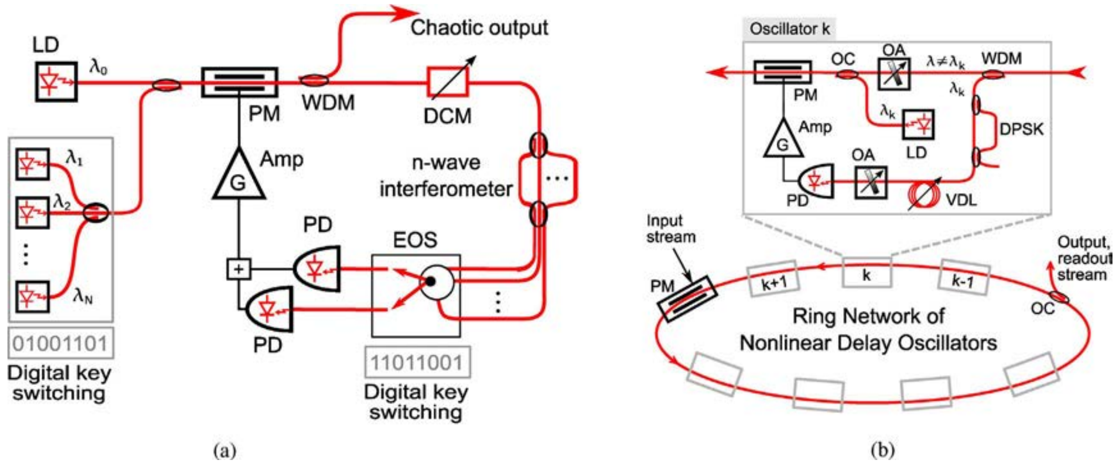

Fig. 4. Advanced phase dynamics architecture. (a) Additional optical processing with analogue and digital keys for enhanced security chaos communications (EOS: electro-optical switch). (b) Ring structure for a networked phase dynamics intended for reservoir computing.

When applying a binary message, the open loop receiver remains synchronized, i.e., $\varphi'(t) \simeq -\varphi(t)$. This locally synchronized chaotic phase modulation φ' is superimposed to the incoming phase modulation $\varphi^\star = \varphi + \varphi_m$ through the receiver EO phase modulation. This leads to a receiver output lightbeam whose phase modulation consists of φ_m only. After chaos cancelation, a standard DPSK lightbeam is thus obtained, which optical spectrum is represented with, and without, chaos cancellation in Fig. 2(c).

The non-authorized receiver is assumed to perform a direct detection without the chaos cancelation process. We switched practically from the authorized [middle blue curve in Fig. 2(c)] to the non-authorized [upper magenta curve in Fig. 2(c)] receiver, simply by disconnecting the fiber seeding the open-loop nonlinear delayed phase chaos cancellation path. The peaks of the data clock are clearly visible, and they are thus not hidden in the chaotic phase modulation. However, it can be seen in the temporal domain in Fig. 3(a) and (c), that chaotic masking is sufficient to strongly perturb the eye diagram, whereas chaos cancelation allows for nicely recovered eyes in Fig. 3(b) and (d). The standard DPSK lightbeam after the receiver phase modulator, is practically processed by a data rate-matched DPSK demodulator, resulting in a binary intensity modulated lightbeam. The latter is finally detected by a photodiode and electronically amplified. When recovering the demodulated binary data stream in the electronic domain for bit error-rate (BER) measurements, we systematically applied for both the authorized and non-authorized receiver, a 7.73 GHz low pass telecom Bessel-Thomson filter, whose cut-off is matched with the spectrum of 10 Gb/s data. This signal is the one used for the eye diagrams in Fig. 3(a)–(d).

When adjusting the operating parameters of the chaos encoding and decoding, one has to deal with a classical trade-off in practical chaos communications: masking (or embedding) efficiency versus decoding quality [20]. Both are tuned by the relative weight of the message phase modulation amplitude ($\eta\pi$ at MΦM, where $\eta = 1$ is the optimum for standard DPSK transmission), and the phase chaos modulation amplitude (tuned by β). As illustrated in Fig. 3, the decoding quality rises significantly when increasing the message amplitude. However, one can notice an impact on the security: the shape of the bits becomes more visible. Nevertheless, even in the case of a high-message amplitude $\eta = 100\%$ and moderate feedback gain $\beta = 2$ the BER of a direct detection is worse than 10^{-1}, while error-free transmission is achieved by the authorized receiver [not represented in Fig. 3(c) since error-free performance is obtained by the authorized decoder, for any η in the presented range]. For $\beta = 4$, a strong nonlinear operation is imposed. This results in a rather amplified parameter mismatch effect for the authorized decoder. For a message relative amplitude set to $\eta = 60\%$, only 10^{-3} BER is obtained, and one would need to push the message amplitude to $\eta = 100\%$ so that it can be properly extracted from the chaotic carrier [BER is then close to 10^{-8} as seen in Fig. 3(e)]. Of course the situation is even worth, as expected, for the unauthorized receiver.

Two successive field experiments were conducted during Summer 2009, for which we mounted the phase chaos encoder and decoder onto A4 breadboards, so that they can be tightly fixed in handluggage-size transportation cases. The first experiments occurred on the “Frères Lumière” all-optical fibre ring network installed in the city of Besançon, France. Only a few additional laboratory devices were required to perform these tests. BERs of 3×10^{-10} and 2×10^{-7} were obtained at 10 Gb/s for $\beta = 2$ and 2.5, respectively, for transmission over the 22 km fibre ring. As already observed with fiber spools in the laboratory, dispersion issues are critical, and successful data recovery was only possible with accurately tuned dispersion compensation modules (in addition to an EDFA for loss compensation). This initial experiment also allowed evaluation of the polarization sensitivity of the link, and polarization control (using standard loop controllers) had to be used appropriately. No other particular fiber channel disturbance was noticed. More specifically, since the transmission is based on fast differential phase modulation, we did not noticed any influence of slowly varying phase perturbations occurring while the optical signal was traveling through the long-fiber channel. Out of channel disturbances, long-term stable operation of the encoding and decoding required the use of control systems for the operating point of the DPSK demodulators.

The second experiment was performed on a more recent and advanced optical network in Athens, Greece [11]. In this case the fiber loop path was close to 120 km and involved two EDFAs and two dispersion compensation units. The measurements were performed in the Telecom Laboratory at the University of Athens, Athens, Greece. We had to properly fix all the fibers before the polarization state was stable enough and did not require any adjustment during several tens of minutes. Under these conditions we could achieve BERs of 10^{-6} and 2×10^{-4} at 10 Gb/s for $\beta = 2$ and 2.5, respectively. By reducing the message bit rate to 3 Gb/s we could achieve BERs of $<10^{-10}$ and 10^{-9} under the same parameter conditions. These first 10 Gb/s field experiments were however not involving all the currently available optical signal processing techniques for 10 Gb/s link optimization. Recently improved transmission conditions in the frame of laboratory experiments, could achieve error-free 10 Gb/s phase chaos communications with a 70 km fiber spool. This recent investigation shows that the performances of phase chaos communication can be even further improved.

IV. CONCLUSION

The proposed phase chaos emitter-receiver setup has demonstrated an efficient and robust solution for optical chaos communications. Its detailed architecture was performed with off-the-shelf components, but the flexibility of this novel approach will allow more complex and dedicated optical processing. Since reliability and efficiency of chaos communications have been now achieved with rather basic architectures, future work will be definitely devoted to the analysis and the enhancement of the related security. Analogue optical signal processing protocols would need to be designed, making use of the numerous available components developed for high-speed optical communications. For example [see Fig. 4(a) for an improved version of the phase chaos generator], advanced processing could be easily implemented inside the chaotic loop: customized multiple wave imbalanced interferometers, highly dispersive elements, dynamically switchable delay lines, additional local secret wavelength source. This would improve the architecture complexity and thus the security, without significantly affecting the setup capability concerning the decoding quality.

Apart from this efficient demonstration of optical chaos communications, we anticipate that the proposed EO phase dynamics principles might also offer interesting potential and features for other recently addressed applications of nonlinear dynamics, such as ultrahigh bit rate random digital sequence generation [21], or optical implementation of reservoir computing [22] [see a proposed ring network principle in Fig. 4(b)].

ACKNOWLEDGMENT

The authors would like to thank city of Besançon, France, for providing the authorization to access the “Lumière” loop network of the city, as well as the University of Athens, Athens, Greece, and ATTIKA Telecom, Athens, Greece, for providing access to part of the metropolitan network of Athens. They are grateful to their industrial partner in the PICASSO Project, Phoenix Photonics, which provided thermally tunable fiber-based DPSK demodulators. They also thank the Region Franche-Comté for its support of advanced optical telecommunication research program within the FEMTO–ST Institute. L. Larger is grateful to the Institut Universitaire de France for its important institutional support.

REFERENCES

[1] L. M. Pecora and T. L. Carroll, “Synchronization in chaotic systems,” *Phys. Rev. Lett.*, vol. 64, no. 8, pp. 821–824, Nov. 1990.
[2] G. D. VanWiggeren and R. Roy, “Communicating with chaotic lasers,” *Science*, vol. 279, no. 3, pp. 1198–1200, Feb. 1998.
[3] J.-P. Goedgebuer, L. Larger, and H. Porte, “Optical cryptosystem based on synchronization of hyperchaos generated by a delayed feedback tunable laser diode,” *Phys. Rev. Lett.*, vol. 80, no. 10, pp. 2249–2252, Jun. 1998.
[4] V. Annovazzi-Lodi, S. Donati, and A. Sciré, “Synchronization of chaotic lasers by optical feedback for cryptographic applications,” *IEEE J. Quantum Electron.*, vol. 33, no. 9, pp. 1449–1454, Sep. 1994.
[5] C. R. Mirasso, P. Colet, and P. Garcia-Fernández, “Synchronization of chaotic semiconductor lasers: Application to encoded communications,” *IEEE Photonics Tech. Lett.*, vol. 8, no. 2, pp. 299–301, Feb. 1996.
[6] A. Uchida, T. Sato, and F. Kannari, “Suppression of chaotic oscillations in a microchip laser by injection of a new orbit into the chaotic attractor,” *Opt. Lett.*, vol. 23, no. 6, pp. 460–462, Mar. 1998.
[7] I. Fischer, Y. Liu, and P. Davis, “Synchronization of chaotic semiconductor laser dynamics on subnanosecond time scales and its potential for chaos communication,” *Phys. Rev. A*, vol. 62, no. 1, pp. 011801-1–011801-4, Jun. 2000.
[8] S. Sivaprakasam and K. A. Shore, “Message encoding and decoding using chaotic external-cavity diode lasers,” *IEEE J. Quantum Electron.*, vol. 36, no. 1, pp. 35–39, Mar. 2000.
[9] H. D. I. Abarbanel, M. B. Kennel, S. Illing, L. Tang, H. F. Chen, and J. M. Liu, “Synchronization and communication using semiconductor lasers with optoelectronic feedback,” *IEEE J. Quantum Electron.*, vol. 37, no. 10, pp. 1301–1311, Oct. 2001.
[10] K. Kusumoto and J. Ohtsubo, “1.5-GHz message transmission based on synchronization of chaos in semiconductor lasers,” *Opt. Lett.*, vol. 27, no. 12, pp. 989–991, June 2002.
[11] A. Argyris, D. Syvridis, L. Larger, V. Annovazzi-Lodi, P. Colet, I. Fischer, J. Garcia-Ojalvo, C. R. Mirasso, L. Pesquera, and A. K. Shore, “Chaos–based communications at high-bit rates using commercial fiber–optic links,” *Nature (London)*, vol. 438, pp. 343–346, Nov. 2005.
[12] A. Argyris, M. Hamacher, K. Chlouverakis, A. Bogris, and D. Syvridis, “Photonic integrated decice for chaos applications in communications,” *Phys. Rev. Lett.*, vol. 100, p. 194101, May 2008.
[13] R. Lavrov, M. Peil, M. Jacquot, L. Larger, V. S. Udaltsov, and J. M. Dudley, “Electro-optic delay oscillator with non-local non linearity: Optical phase dynamics, chaos, and synchronization,” *Phys. Rev. E*, vol. 80, pp. 026207-1–026207-9, Aug. 2009.
[14] L. Larger, J.-P. Goedegbuer, and V. S. Udalsov, “Ikeda-based nonlinear delayed dynamics for application to secure optical transmission systems using chaos,” *C. R. Phys. 4*, vol. 5, no. 6, pp. 669–681, Jul. 2004.
[15] M. Mackey and L. Glass, “Oscillation and chaos in physiological control systems,” *Science*, vol. 197, pp. 287–288, Jul. 1977.
[16] K. Ikeda, “Multiple-valued stationary state and its instability of the transmitted light by a ring cavity system,” *Opt. Commun.*, vol. 30, no. 3, pp. 257–261, Aug. 1979.
[17] A. Neyer and E. Voges, “Dynamics of electrooptic bistable devices with delayed feedback,” *IEEE J. Quantum Electron.*, vol. 18, no. 12, pp. 2009–2015, Dec. 1982.
[18] V. Udaltsov, L. Larger, J.-P. Goedgebuer, J.-B. Cuenot, P. Levy, and W. T. Rhodes, “Cracking chaos-based encryption systems ruled by nonlinear time delay differential equations,” *Phys. Lett. A*, vol. 308, pp. 54–60, Jan. 2003.
[19] Y. C. Kouomou, P. Colet, L. Larger, and N. Gastaud, “Mismatch-induced bit error-rate in optical chaos communication using semiconductor lasers with electro-optical feedback,” *IEEE J. Quantum Electron.*, vol. 41, no. 2, pp. 156–163, Feb. 2005.
[20] L. Larger, J.-P. Goedgebuer, and F. Delorme, “Optical encryption system using hyperchaos generated by an optoelectronic wavelength oscillator,” *Phys. Rev. E*, vol. 57, no. 6, pp. 6618–6624, Jun. 1998.
[21] A. Uchida, K. Amano, M. Inoue, K. Hirano, S. Naito, H. Someya, I. Oowada, T. Kurashige, M. Shiki, S. Yoshimori, K. Yoshimura, and

P. Davis, “Fast physical random bit generation with chaotic semiconductor lasers,” *Nature Photon. (London)*, vol. 2, no. 728–732, Dec. 2008.

[22] W. Maass, T. Natschläger, and H. Markram, “Real–time computing without stable states: A new framework for neural computation based on perturbations,” *Neural Comput.*, vol. 14, no. 11, pp. 2531–2560, 2002.